

Effect of Organic Surfactant on Femtosecond Solvation Dynamics at the Air–Water Interface

Alexander V. Benderskii and Kenneth B. Eisenthal*

Department of Chemistry, Columbia University, New York, New York 10027

Received: July 18, 2000; In Final Form: October 6, 2000

Solvation dynamics at an air–water interface covered with a Langmuir monolayer of a neutral surfactant stearic acid $\text{CH}_3(\text{CH}_2)_{16}\text{COOH}$ was measured using femtosecond pump–probe spectroscopy of a molecular probe, coumarin 314. The second harmonic generation was used as a surface-specific ultrafast probe. The results are compared with the solvation dynamics measured for the same probe molecule at the air–water interface without the surfactant. The overall solvation time in the presence of the fatty acid monolayer ($\tau_s = 400 \pm 60$ fs) differs from that at the air–water interface, where two components $\tau_1 = 250 \pm 60$ fs and $\tau_2 = 1250 \pm 80$ fs were obtained, with an amplitude weighted average solvation time of $\tau_s = 850 \pm 70$ fs. These results are in agreement with bulk studies of coumarins in water. The different solvation dynamics at the surfactant modified interface is attributed to rearrangement of the hydrogen bonding network of water molecules near the interface due to interactions with the hydrophilic carboxyl group of the surfactant.

Introduction

Liquid interfaces host a variety of chemical processes important in areas ranging from cell biology and medical applications, to electrochemistry and heterogeneous catalysis, to semiconductor processing and solar energy conversion. Understanding the physical and chemical properties of liquid interfaces thus represents both a fundamental scientific challenge and a potential for break-through advances in technology. Besides the broken symmetry, liquid–liquid, liquid–solid, and biological (e.g., cell membrane) surfaces are often characterized by specific interactions present at the interfaces. Solvation properties in general describe rearrangement of the solvent molecules to best accommodate the solute, thus minimizing the total free energy. Similar to the bulk processes, energetics and dynamics of interfacial solvation are expected to have a profound effect on adsorption, chemical equilibria, as well as on reaction dynamics at liquid interfaces.¹

Many factors contribute to the solvation energy in the general case, including specific local solute–solvent interactions such as hydrogen bonding, as well as nonspecific long range electrostatic and van der Waals forces. When a charge redistribution occurs in the solute immersed in a polar solvent, the dominant contribution to the solvation free energy is often due to the dielectric relaxation of the environment brought by the reorientation of the dipolar solvent molecules. Apart from the instantaneous electronic polarizability response, all contributions involve orientational and translational motions of the solvent molecules surrounding the solute, which occur on a longer time scale. The delayed solvent response, which has been determined by experimental studies of femtosecond solvation dynamics, can have a crucial influence on the chemical reaction rates in liquids, especially charge-transfer processes.

Water, the most important of the solvents, has been extensively studied both theoretically and experimentally. The relaxation involves the complex collective motion of a large ensemble of water molecules, whose individual motions are strongly coupled by hydrogen bonding, dipole–dipole interac-

tions, etc., presenting a challenging fundamental problem for condensed phase theory. Owing to its small size, water is the fastest of all studied solvents. Both experiments and computer simulations have shown a bimodal response to a sudden change in the solute charge distribution.^{2,3,4} The fast inertial component, which has been identified mainly with librations of water molecules, accounts for $\sim 50\%$ of the solvation free energy and proceeds on a time scale shorter than 30 fs, faster than the experimental time resolution in most cases. The slower diffusive component is often represented by a biexponential decay with the characteristic times of ~ 250 fs and ~ 1.2 ps, and the amplitude-averaged solvation time τ_s from 600 to 900 fs, depending on the probe molecule employed for the measurement.² This relaxation mode has been assigned to the coupled rotations and translational motions associated with rearrangement of the hydrogen bonding network.

It is a fascinating question how does solvation at an interface differ from the bulk liquid response. Consider, for example, biological systems, where a host of vital reactions occur at membranes, liposome bilayers, or micelle surfaces, or near proteins or DNA molecules.⁵ Many biologically important processes involve intra- and intermolecular electron and proton transfer (at least as one of the steps), whose rates are governed by the dynamical solvent reorganization triggered by the charge redistribution in the reactant species. Examples include the various steps of photosynthesis, photoinduced charge-transfer reactions involved in vision, and many proteins whose primary function is electron and proton transfer (e.g., cytochrome, hemoglobin charge transfer in respiration process, etc.).

Intuitively, one might expect that the specific interactions at the interface would bind the interfacial molecules, resulting in slower dynamics. A manifestation of this was observed as increased friction at a boundary between water and organic solvents, air–water, and silica–water interfaces on picosecond time scale, witnessed by the slowed isomerization of malachite green,⁶ as well as slowing of molecular rotational diffusion of rhodamine 6G⁷ and coumarin 314⁸ at the air–water interface relative to bulk water. A similar effect on solvation dynamics

was observed in reverse micelles, where reorientation of the water molecules inside the micelle is severely hindered by the geometrically restricted environment.^{9,10} On the other hand, interactions of the water molecules with the surfactant can break the hydrogen bonding network close to the interface, allowing them to move more freely. This mechanism, supported by theoretical modeling,¹¹ was employed recently to explain the observed faster overall solvation decays measured at the surface of ZrO₂ nanoparticles.¹² Finally, if the surface is charged, the interfacial electric field induces additional orientation of the solvent molecules,^{13,14} which may also affect the solvation properties.

Several experimental methods have been employed to measure dynamical properties of liquid water.^{2,15} Perhaps the most straightforward approach, and the one that best illustrates the paradigm of solvation dynamics, is to use an ultrashort laser pulse to suddenly induce electronic excitation of a probe solute molecule, changing its charge or dipole moment, then monitor the energy of the excited state in real time using another femtosecond pulse. In the bulk solvents, this is usually accomplished by following the time-dependent fluorescence Stokes shift of an appropriately chosen dye in a fluorescence up-conversion setup.^{2,3}

Solvation dynamics at the air–water interface was measured in recent studies.^{16,17,18} Time-resolved second harmonic generation (TRSHG) was used as a surface-specific probe of the coumarin 314 adsorbate, using ultrafast femtosecond laser methods. It should be noted that the reorientation at the air–water interface occurs on a much longer time scale, ~ 300 ps for coumarin 314.⁸ Thus, the subpicosecond dynamics that we observe in these experiments is readily separated from the reorientation dynamics. The solvation dynamics time scales at the interface were found to be similar to the bulk values of similar coumarins.^{2,3} One possibility to explain these results is that the long-range interactions, i.e., the solvation not only from the first shell, but the second water shell and further shells, make key and bulklike contributions to the solvation dynamics. Support for this is found in experiments,¹⁹ which showed that the polarity of water interfaces ranging from the air–water to several oil–water interfaces could be accurately predicted from polarity measurements of the bulk media that define the interface.

Because the air–water interface can be easily covered with various surfactants, they present the possibility to isolate and study the effect of the surfactant on the interfacial dynamics. In the present report, we investigate the effect of a neutral monolayer of a long-chain carboxylic acid on solvation dynamics at the air–water interface.

Water insoluble long-chain amphiphilic compounds are known to form well-ordered Langmuir monolayers at the air–water surface, with the hydrophilic headgroups immersed into the water phase and the hydrophobic tails pointing in the air.²⁰ Orientational ordering of pentadecanoic acid nearly perpendicular to the interface was explicitly demonstrated in a vibrational sum-frequency generation (SFG) surface spectroscopic study.²¹ Studies of these two-dimensional systems, their states and phase transitions have been an active area of research since the beginning of the century.^{22–24} Of particular importance is their close resemblance to biological interfaces, since many of the latter are composed of long-chain organic molecules with hydrophilic groups pointing into the water phase.

The present experimental system has a number of advantages. (1) The surfactants (both the dye and the organic monolayer) can be well characterized by surface tension measurements²⁰

as well as surface spectroscopy.^{21,25} (2) The adsorption, orientation, and transition energies of the dye molecule serving as a probe of solvation dynamics can be well determined by molecular orientation measurements and surface-specific SH spectroscopy to aid interpretation of the time-resolved studies. (3) Dynamics with and without the monolayer can be measured and direct comparison can be made to demonstrate the effect of the surfactant on the dynamics of water molecules near the interface. (4) Because the interface is planar, no geometric restrictions arise, as in the case of micelles, or other microscopic particles. The current approach therefore makes it possible to separate the effects of different surface-specific interactions on solvation dynamics. Particularly in the present case, a relatively low surfactant surface coverage ($200 \text{ \AA}^2/\text{molecule}$) can amplify the effect of the specific interaction between water molecules near the interface with the hydrophilic carboxyl groups. (5) Because many species are known to form Langmuir monolayers on the water surface, the method can be extended to study the effect of different functional groups. (6) Both neutral and charged monolayers can be prepared (e.g., by adjusting acidity of the underlying solution to ionize the surfactant) to study the effect of the interfacial electric field on the static and dynamical solvation properties.

This paper reports the first measurement of femtosecond solvation dynamics at an organic Langmuir monolayer interface. Our results demonstrate that even a relatively small amount of a long-chain carboxylic acid surfactant has a significant effect on the dynamics. With respect to the air–water interface, the faster component (250 fs) seems to increase to 400 fs at the monolayer–water interface, whereas the slower component (1250 fs) is suppressed. This results in a shorter overall solvation time, by a factor of 2, in the presence of the hydrophilic neutral surfactant. This effect is interpreted as rearrangement of the hydrogen bonding network of water molecules near the interface by hydrophilic interactions with the carboxyl headgroup of the surfactant. The modified hydrogen bonding structure is characterized by the different dynamics of librational, orientational, and translational relaxation motions.

Experimental Section

Coumarin 314 (laser grade) was purchased from Acros and used without further purification. Saturated solutions (at 20° C) were prepared in deionized, doubly distilled water with pH = 3.0, adjusted by adding HCl. The water-soluble ester, coumarin 314, is insensitive to the solution pH in the range 3.0–11.0, as verified by UV–vis spectroscopy. The peak absorbance at $\lambda_{\text{max}} = 448 \text{ nm}$ was $A = 0.7$, corresponding to the dye concentration $C = 15 \text{ }\mu\text{M}$. The solution was contained in a shallow Teflon beaker, and SHG experiments were conducted using reflection of the probe laser beam off the free surface of the solution.

Langmuir monolayers were prepared by spreading a 0.1 mM solution of stearic acid $\text{CH}_3(\text{CH}_2)_{16}\text{COOH}$ (Aldrich) in hexane on the surface of the sample in the beaker using a Hamilton microsyringe. The spreading solvent (hexane) evaporates in less than one minute, but typically 20–30 min are required to form a uniform monolayer of the fatty acid due to slow surface diffusion.²⁶ The monolayers are neutral because the pH = 3.0 of the solution is well below the $\text{p}K_{\text{a}} \approx 5.0$ value of the stearic acid.

The Langmuir monolayers of stearic acid on water surface are known to undergo a first order 2D gas–liquid-phase transition at the surface coverage of $A = 24 \text{ \AA}^2/\text{molecule}$.²⁰ The presence of the surface-active C314 at the interface significantly

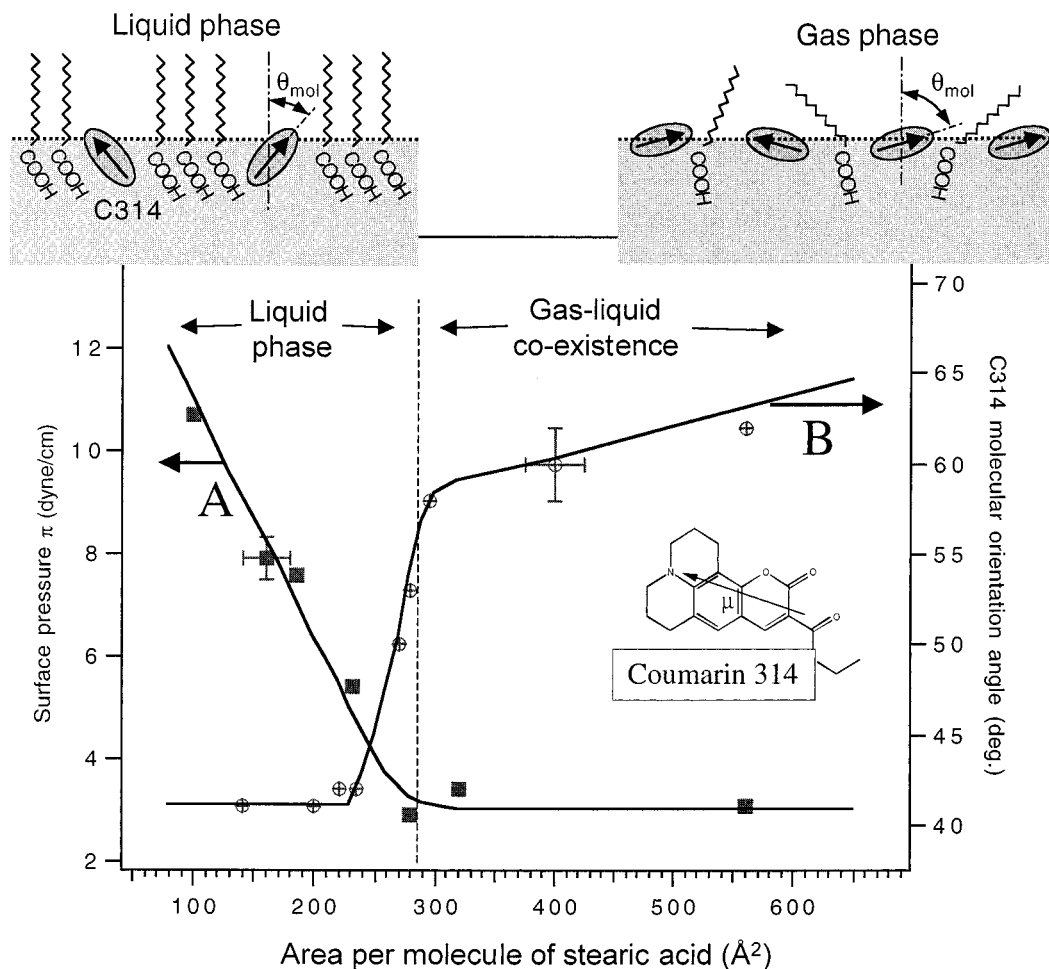


Figure 1. (A) Filled squares: surface pressure – surface coverage ($\pi - A$) 2D phase diagram of the stearic acid $\text{CH}_3(\text{CH}_2)_{16}\text{COOH}$ monolayer on saturated ($15 \mu\text{M}$) solution of coumarin 314 in water ($\text{pH} = 3.0$). (B) Open circles: molecular angle of the coumarin 314 adsorbed at air–water interface in the presence of the stearic acid monolayer, measured using the second harmonic null-angle technique.

shifts this phase transition, to $A = 260 \text{ \AA}^2/\text{molecule}$, as demonstrated by the surface pressure measurements performed on the saturated C314 solution using a Wilhelmy plate setup (Figure 1A). This effect has been observed previously for other surface-active solutes (e.g., *p*-nitrophenol^{26,27}), and can be rationalized as competition of the two surfactants for the available surface sites. For the solvation dynamics experiments, $14 \mu\text{L}$ of the 0.1 mM stearic acid/hexane solution was spread on the surface of the beaker, corresponding to the surface coverage $A = 200 \text{ \AA}^2/\text{molecule}$, in the liquid region just below the gas–liquid-phase transition. This minimizes fluctuations of the SH signal due to “islands” of the surfactant present in the gas–liquid coexistence region.

The setup for time-resolved SHG was described in detail previously.^{8,17} Briefly, a regeneratively amplified Ti–sapphire laser system (Clark-MXR) produces 120 fs , 1 mJ pulses, at the fundamental wavelength $\lambda = 850 \text{ nm}$, at 1 kHz repetition rate. A small portion of the output was frequency doubled in a BBO crystal to produce $1 \mu\text{J}$ pump pulses at 425 nm . A polarizer followed by a half-wave plate were used to control polarization of the pump (S or P). $70 \mu\text{J}$ of the fundamental output were separated to use as a probe beam. Both pump and probe beams were directed onto the sample surface at 70° incidence angle (from normal), and focused by two 1 m f.l. lenses to 0.5 mm diameter spot at the surface. Typically, the probe beam was polarized at 45° , and (S)-analyzer was used to select the $\chi_{xzxx}^{(2)}$ element of the second-order nonlinear susceptibility tensor.²⁵

The pump and probe beams were separated by a small angle, 5° , in the horizontal plane to minimize loss of temporal resolution. This enables spatial separation of the generated second harmonic signal from the pump light. A long-pass wavelength colored glass filter was placed in the probe beam immediately before the sample to block any spurious SH, and a short-pass blue filter was placed immediately after the sample surface to block the reflected fundamental wavelength. The generated SH beam (collinear with the reflected probe beam) was dispersed through a $1/4 \text{ m}$ monochromator (Jarrel Ash) and detected by a Hamamatsu PMT (model R4220P). Four irises (1 mm) were positioned along the 1 m path of the collimated SH signal from the sample to the monochromator, reducing the background from the scattered pump light (at the same frequency as the generated SH) to less than 1%. Typically, on the order of 10 SH photons per laser shot were collected, thus single photon counting was not required. The PMT signal was integrated and averaged using a Stanford Research Systems boxcar, and recorded by a computer (National Instruments A/D board) that controlled the delay between the pump and probe pulses via a stepper-motor driven translational stage (Klinger).

Zero delay and pump–probe cross-correlation were recorded using sum frequency generation on the sample surface. The measured instrument response function (cross-correlation fwhm $\tau_0 = 180 \text{ fs}$) was used in fitting the initial drop in the transients as described in the next section. To avoid local heating, desorption, and bleaching of the dye by the one-photon resonant

pump beam, the sample beaker was rotated at 4 rpm with the focal spot of the laser 1.5 cm off center. With this precaution, no sample degradation was observed over the course of an experiment.

Results and Discussion

We begin by characterizing the effect of the stearic acid monolayer on the orientation and static (equilibrium) solvation of the ground electronic state coumarin 314 adsorbed at the air–water interface. The molecular orientation of C314 was measured using the second harmonic null angle technique.^{28,29} At the air–water interface, in the absence of stearic acid, C314 has an orientation $\theta_{\text{mol}} = 70 \pm 3^\circ$ with respect to the normal, assuming a narrow distribution, that is, lying almost flat on the surface. The fatty acid surfactant has a pronounced effect on the molecular orientation of the C314 adsorbed at the interface (Figure 1B). Above the phase transition, at stearic acid surface coverage $A > 260 \text{ \AA}^2/\text{molecule}$, or, equivalently, at surface concentrations less than $3.8 \times 10^{13} \text{ cm}^{-2}$, the molecular angle θ_{mol} of C314 decreases monotonically with the surfactant coverage. We note, however, that in this gas–liquid coexistence region, the surface consists of isolated “islands” of the liquid phase separated by the gas phase, and that the molecular angle represents an average over a broad inhomogeneous orientational distribution. The molecular angle drops sharply to $\theta_{\text{mol}} = 41 \pm 3^\circ$ at the phase transition to the liquid phase, and is independent of the surfactant concentration below the transition ($A < 260 \text{ \AA}^2/\text{molecule}$). It has been shown that in the liquid 2D phase, the structure of the surfactant monolayer is uniform and highly ordered,²⁰ with the long-chain fatty acids oriented nearly normal to the surface.²¹

The total second harmonic signal (measured without the analyzer) from adsorbed C314 is a factor of 4 weaker in the presence of the monolayer than at the surfactant-free air–water interface. By not placing an analyzer in the SH signal beam, we are collecting all of the SH light generated by the C314 at the surface, thus reducing any possible effects due to change in orientation of the chromophore. Because the total SH intensity is proportional to the dye surface concentration squared, this indicates that the monolayer reduces the C314 surface concentration by a factor of 2, i.e., the stearic acid displaces surface coumarin, pushing it into solution. Both in the absence and in the presence of the monolayer, the surface concentration of C314 is less than $2.5 \times 10^{13} \text{ cm}^{-2}$.

Surface second harmonic spectroscopy of the C314 adsorbed at the interface was performed using an unamplified Ti–sapphire oscillator (Spectra-Physics Tsunami) tunable from 790 to 900 nm. The surface spectra (Figure 2, B, C) show the shift of the $S_0 \rightarrow S_1$ electronic transition energy, reflecting a different solvation environment at the interface.¹⁸ The absorption maximum of C314 in bulk water is at $\lambda_{\text{max}} = 448 \text{ nm}$ and fwhm of the transition is $\sim 50 \text{ nm}$ (Figure 2, A), whereas at the air–water interface, the SH signal peaks at 423 nm and fwhm = 14 nm. This corresponds to the ground-to-excited-state transition energy of $\lambda_{\text{max}} \sim 419 \text{ nm}$, a correction arising from interference of the resonant and nonresonant terms in the nonlinear response.¹⁹ The shift reflects reduced polarity of the air–water interface compared to the bulk water.

A monolayer of stearic acid ($A = 200 \text{ \AA}^2/\text{molecule}$) shifts the surface spectrum to the red, to 432 nm, corresponding to the transition energy $\lambda_{\text{max}} \sim 428 \text{ nm}$, and broadens it to fwhm = 20 nm (Figure 2B). The spectrum clearly indicates that the dye experiences an increased polarity. This can be a result of the direct solvation of coumarin by the stearic acid,

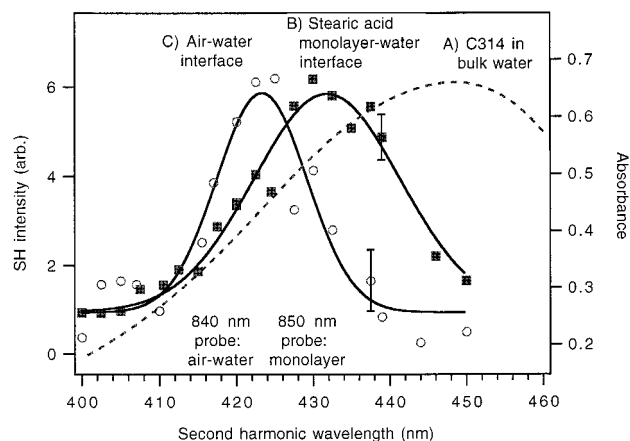


Figure 2. (A) Dashed line: absorption spectrum of coumarin 314 dissolved in bulk water (pH = 3.0). B) Filled squares: second harmonic spectrum of coumarin 314 adsorbed at air–water interface covered with a monolayer of stearic acid ($A = 200 \text{ \AA}^2/\text{molecule}$). Solid line shows the fit to a Gaussian with the peak wavelength 432 nm and fwhm = 20 nm. C) Open circles: second harmonic spectrum of coumarin 314 adsorbed at the air–water interface. Solid line: Gaussian fit with the peak at 423 nm and fwhm = 14 nm.

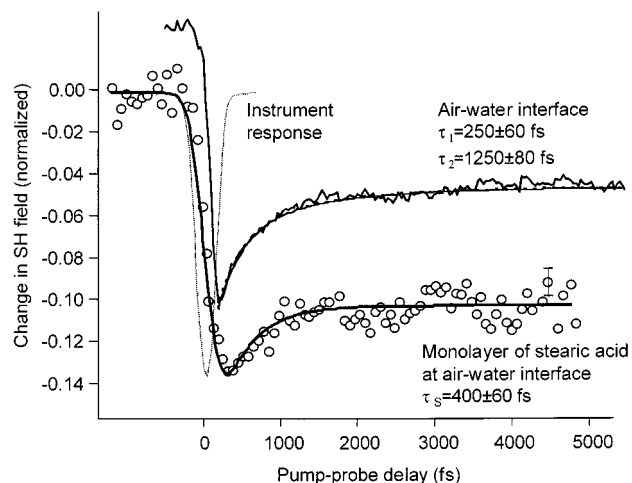


Figure 3. Lower trace: pump–probe transient second harmonic signal of the coumarin 314 at air–water interface covered with a monolayer of stearic acid ($A = 200 \text{ \AA}^2/\text{molecule}$). Probe wavelength is 850 nm ($\lambda_{\text{SH}} = 425 \text{ nm}$), XZX element of the $\chi^{(2)}$ is detected. Pump wavelength is 425 nm. Solid line shows a single-exponential fit of the interfacial solvation dynamics with a time constant $\tau_s = 400 \pm 60 \text{ fs}$. The pump–probe cross-correlation function is shown by dashed line at $t = 0$. Upper trace: Solvation dynamics measured at air–water interface without surfactant.¹⁸ Solid line shows biexponential fit with $\tau_1 = 250 \pm 60 \text{ fs}$ and $\tau_2 = 1250 \pm 80 \text{ fs}$.

which increases the effective polarity of the interface. Another possible explanation is that the adsorbed C314 is pushed deeper into the water phase by the fatty acid surfactant, and is thus more fully solvated by the bulk water.

Figure 3A shows the real-time femtosecond solvation dynamics of the interfacial C314 at the stearic acid monolayer ($A = 200 \text{ \AA}^2/\text{molecule}$) measured in a TRSHG pump–probe experiment. One-photon resonant electronic excitation $S_0 \rightarrow S_1$ at $t = 0$ is accomplished by a 425 nm pump pulse. The initial 10% bleach in the SH signal represents population transfer from the ground to the excited state. The second harmonic probe ($\lambda_{\text{probe}} = 850 \text{ nm}$) monitors the excited state of the coumarin as its energy is lowered by solvation, which shifts it to the red and away from the resonance, thereby decreasing the excited-state nonlinearity. This appears as partial recovery of the signal,

owing to less cancellation between the coherent SH fields generated by the ground and excited-state dye molecules.⁸

The transients were fit to extract the characteristic solvation response time τ_s . The initial drop of the SH signal is represented as $\text{erf}(t/\tau_0)$, an integral of the Gaussian instrument response function with the time constant $\tau_0 = 180$ fs measured by pump–probe cross-correlation. The subsequent recovery is fit to a single exponential

$$S(t) = 1 - \frac{A_1}{2} [1 + \text{erf}(t/\tau_0)] \left[1 - \frac{A_2}{A_1} \{1 - \exp(-t/\tau_s)\} \right]$$

with three fitting parameters: amplitudes of the initial drop (A_1) and partial recovery (A_2), and τ_s . The solvation dynamics measured at the stearic acid monolayer can be well fit by a single exponential with a time constant $\tau_s = 400 \pm 60$ fs. We note that approximately ± 50 fs uncertainty in the decay time originates from the finite instrument temporal resolution because the extracted decay rate is somewhat dependent on the fitting of the initial drop. Identical dynamics within experimental uncertainty were measured for S- and P-polarized pump.

The probe wavelength $\lambda_{\text{probe}} = 850$ nm ($\lambda_{\text{SH}} = 425$ nm) used in the fatty acid monolayer measurements is blue-shifted from the peak wavelength of 432 nm and is located on the shoulder of the SH spectrum (Figure 2). The dynamics measured at this wavelength is expected to faithfully represent the solvation dynamics, as the excited-state transition energy is lowered by solvation and shifts to the red, away from the probe wavelength. In other words, the chosen probe wavelength is a linear wavelength for the solvation dynamics.¹⁸ At the linear probe wavelength, the SH intensity is linearly proportional to the solvation coordinate, therefore the TRSHG experiment directly measures the solvation dynamics. Identical dynamics within experimental uncertainty were measured for S- and P-polarized pump, which also supports the assumption that the chosen wavelength is close to the linear wavelength.

Experiments at the stearic acid covered interface were performed using different probe wavelengths within 830–850 nm range ($\lambda_{2\omega} = 415, 420, \text{ and } 425$ nm). The obtained solvation times are essentially independent of the probe wavelength, within the 10–15% experimental accuracy, which is another indication that we are in the linear wavelength region. This shows that the measured solvation dynamics time is not sensitive to the exact choice of the probe wavelength in this wavelength region.

Our results demonstrate that the stearic acid monolayer induces significant changes in both static and dynamic solvation at the air–water interface. The red shift of the surface SH spectrum of the C314 probe, from 423 nm at the air–water interface to 432 nm at the stearic acid monolayer, indicates an increased polarity of the equilibrium solvation environment at the surfactant-modified interface. Dynamics of interfacial solvation is also significantly affected by the stearic acid surfactant. In a previous study, it was inferred that the solvation dynamics of C314 at the air–water interface is very similar to that in the bulk water.^{17,18} Although the finite temporal resolution did not allow observation of the ultrafast inertial component (< 30 fs), a biexponential decay was obtained with two time constants $\tau_1 = 250 \pm 60$ fs and $\tau_2 = 1250 \pm 80$ fs,¹⁸ which agrees well with the biexponential diffusive solvation observed in the bulk.² On the contrary, at the stearic acid monolayer interface, we observe a single-exponential decay of 400 ± 60 fs. While it is comparable to (although somewhat slower than) the faster $\tau_1 = 250$ fs component at the air–water interface, it appears

that the slower $\tau_2 = 1250$ fs component is suppressed by the stearic acid surfactant. The net result is an overall faster solvation compared to the air–water interface, where the amplitude-averaged solvation time is $\tau_s = 850 \pm 70$ fs.

While the temporal resolution of our current setup does not allow observation of the ultrafast (< 30 fs) inertial solvation component, we find that the slower diffusive solvation component is significantly modified by the presence of a Langmuir monolayer of stearic acid at the air–water interface. Numerous theoretical efforts associate this diffusive component with hindered rotations and translations of water molecules involving the breaking of hydrogen bonds between them.^{3,30} A plausible explanation of the observed effect on the dynamics is that the water molecules interact with the hydrophilic carboxyl head-groups of the fatty acid and this results in rearrangement of the network of water–water hydrogen bonds near the interface.^{14,31,32} The rearranged network has different dynamical characteristics in terms of librations, rotations, and translations of the water molecules.

To help substantiate our interpretation, different experimental and theoretical studies present evidence that the network of hydrogen bonded water molecules near an interface can be significantly altered by the specific interfacial interactions that are absent in the bulk. In situ X-ray scattering from an Ag electrode interface¹³ showed greatly increased density and structure in the first three layers near the water–metal interface, markedly different from the bulk properties. Vibrational sum frequency generation (VSFG) spectroscopy in the OH stretching region was used to study the interfacial water structure,³² suggesting that various surfactants (e.g., pentadecanoic acid¹⁴ or a phospholipid monolayer³¹) as well as solid interfaces³² can significantly alter the hydrogen bonding patterns of water. Molecular dynamics simulations also indicate the reduced hydrogen bonding at a surface of cylindrical pores, with resulting faster relaxation.¹¹

Although understanding the solvation dynamics of bulk water has been subject of a massive theoretical effort, including both analytical models and computer simulations,^{3,33,30} at present there are very few models of interfacial solvation dynamics pertinent to the effect of the stearic acid monolayer described here. The connection between the water structure near the interface and dynamical properties such as polar solvation response time may be nontrivial. In general, one would expect that, owing to the additional interactions imposed by the surfactant, the water molecules near the interface are more restricted in their motions. This would lead to both smaller amplitude of the solvation response (lowering of the free energy of solvation) and slower relaxation times. However there may be several temporal components whose amplitudes add to the overall solvation response, and some of them may be suppressed more than the others. Thus if the slower components are suppressed, the overall solvation response will appear faster, while if the surface quenches the faster component, the overall solvation time will increase.

A pronounced slowing of the solvation dynamics was observed by several research groups in reverse micelles, where, due to their small size, the motion of the water molecules in the proximity of the micelle wall is highly restricted.^{9,10} On the other hand, an opposite effect on solvation dynamics was recently observed at the surface of ZrO₂ nanoparticles, where the overall solvation time is faster than in the bulk water.¹² Although the ZrO₂ surface (at a slightly acidic pH used in that experiment) is terminated by the hydrophilic OH groups, and is therefore somewhat similar to our system, several mechanisms

could affect the solvation at the nanoparticle surface, as was discussed in ref 12. Because the solution pH was below the point of zero charge, the particles are negatively charged, and therefore the water molecules may be pre-aligned by the interfacial electric field.^{13,14} Due to the presumably high surface concentration of the polar terminal hydroxyl groups on the ZrO₂ surface, their fast librational motions may contribute to the interfacial solvation dynamics in addition to surface water motion, thus causing a faster overall solvation time. Finally, a geometric effect of the solid nanoparticle surface which partially blocks the solvent sensed by the probe dye molecule, has to be taken into account. Thus, as noted in the ZrO₂ work, it is uncertain as to whether the hydrophilic interfacial interactions were the dominant factor modifying the solvation dynamics.

The experiments described in the present paper measure the solvation dynamics at the planar air–water interface with and without the neutral fatty acid monolayer. A direct comparison can be made, thus isolating the effect of the hydrophilic surfactant on the solvation dynamics. Because the aqueous dipolar solvation of the probe dye is dominated by libration, reorientation, and translation of water molecules, we attribute the observed effect to the hydrophilic interactions between carboxyl headgroups of the stearic acid surfactant and water molecules near the interface.

Conclusion

The effect of a Langmuir monolayer of fatty acid on static solvation properties as well as femtosecond solvation dynamics at a planar air–water interface was investigated using second harmonic generation as a surface-specific probe. The solvation dynamics is significantly modified in the presence of the stearic acid monolayer. A single-exponential decay is observed with a time constant of $\tau_S = 400 \pm 60$ fs, while at the air–water interface without any surfactant, a bimodal solvation with $\tau_1 = 250 \pm 60$ fs and $\tau_2 = 1250 \pm 80$ fs has an amplitude averaged time of 850 ± 70 fs. The overall solvation response thus appears a factor of 2 faster at the stearic acid monolayer interface. This effect is attributed to rearrangement of the hydrogen bonding network of water molecules near the interface by the hydrophilic interaction with the carboxyl headgroups of the surfactant, which suppresses the slower solvation component, i.e., allows the water molecules to move more freely. The Langmuir monolayer studied here mimics specific interfacial interactions relevant to many biological interfaces such as liposomes, micelles, and cell membranes, which are often comprised of long-chain lipid molecules with hydrophilic groups at the surface. Our results suggest that the hydrogen bonding interfacial interactions can significantly influence the dynamical solvent relaxation properties at a variety of biological interfaces. This has potential implications for many important processes at interfaces, such as charge transfer, which are controlled by the solvation dynamics.

Acknowledgment. The authors gratefully acknowledge the National Science Foundation for their support.

References and Notes

- (1) Eienthal, K. B. *Acc. Chem. Res.* **1993**, *26*, 636; *J. Phys. Chem.* **1996**, *100*, 12997.
- (2) Barbara, P. F.; Jarzaba, W. *Adv. Photochem.* **1990**, *15*, 1.
- (3) Maroncelli, M. *J. Mol. Liquids* **1993**, *57*, 1.
- (4) Jimenez, R.; Fleming, G. R.; Kumar, P. V.; Maroncelli, M. *Nature* **1994**, *369*, 471.
- (5) Nandi, N.; Bagchi, B. *J. Phys. Chem. B* **1997**, *101*, 10954; *ibid. A* **1998**, *102*, 8217.
- (6) Shi, X.; Borguet, E.; Tarnovsky, A.; Eienthal, K. B. *Chem. Phys.* **1996**, *205*, 167.
- (7) Castro, A.; Sitzmann, E. V.; Zhang, D.; Eienthal, K. B. *J. Phys. Chem.* **1991**, *95*, 6752.
- (8) Zimdars, D.; Dadap, J. I.; Eienthal, K. B.; Heinz, T. F. *J. Phys. Chem. B* **1999**, *103*, 3425.
- (9) Levinger, N. E.; Riter, R. E. In *Liquid Interfaces in Chemical, Biological, and Pharmaceutical Applications*; Volkov, A. G., Ed.; Marcell Dekker: New York, 2000 (in press).
- (10) (a) Pant, D.; Riter, R. E.; Levinger, N. E. *J. Chem. Phys.* **1998**, *109*, 9995. Riter, R. E.; Undiks, E. P. (b) Levinger, N. E. *J. Am. Chem. Soc.* **1998**, *120*, 6062. (c) Riter, R. E.; Willard, D. M.; Levinger, N. E. *J. Phys. Chem. B* **1998**, *102*, 2705.
- (11) Harting, C.; Witschel, W.; Spohr, E. *J. Phys. Chem. B* **1998**, *102*, 1241.
- (12) Pant D.; Levinger, N. E. *Chem. Phys. Lett.* **1998**, *292*, 200; *J. Phys. Chem. B* **1999**, *103*, 7846.
- (13) Toney, M. F.; Howard, J. N.; Richer, J.; Borges, G. L.; Gordon, J. G.; Melroy, O. R.; Wiesler, D. G.; Yee, D.; Sorensen, L. B. *Nature* **1994**, *368*, 444.
- (14) Gragson, D. E.; McCarthy, B. M.; Richmond, G. L. *J. Phys. Chem.* **1996**, *100*, 14272.
- (15) Castner, E. W.; Chang, Y. J.; Chu, Y. C.; Walrafen, G. E. *J. Chem. Phys.* **1995**, *102*, 653.
- (16) Zimdars, D.; Dadap, J. I.; Eienthal, K. B.; Heinz, T. F. *Chem. Phys. Lett.* **1999**, *301*, 112.
- (17) Zimdars, D.; Eienthal, K. B. *J. Phys. Chem. A* **1999**, *103*, 10567.
- (18) Zimdars, D.; Eienthal, K. B., submitted for publication.
- (19) Wang, H.; Borguet, E.; Eienthal, K. B. *J. Phys. Chem. A* **1997**, *101*, 713; *J. Phys. Chem. B* **1998**, *102*, 4927.
- (20) Gaines, G. L., Jr. *Insoluble Monolayers at Liquid–Gas Interfaces*; Interscience Publishers, J. Wiley & Sons: New York, 1966.
- (21) Guyot-Sionnest, P.; Hunt, J. H.; Shen, Y. R. *Phys. Rev. Lett.* **1987**, *59*, 1597.
- (22) Lord Rayleigh, *Philos. Mag.* **1899**, *48*, 437.
- (23) Langmuir, L. *J. Am. Chem. Soc.* **1917**, *39*, 1848.
- (24) Adamson, A. W. *Physical Chemistry of Interfaces*; Wiley-Interscience: New York, 1982.
- (25) (a) Shen, Y. R. *The Principles of Nonlinear Optics*; Wiley-Interscience: New York, 1984. (b) Heinz, T. F. In *Nonlinear Surface Electromagnetic Phenomena*; Ponath, H.-E., Stegeman, G. I., Eds.; Elsevier: Amsterdam, 1991; p 353.
- (26) Zhao, X.; Goh, M. C.; Subrahmanyam, S.; Eienthal, K. B. *J. Phys. Chem.* **1990**, *94*, 3370.
- (27) Zhao, X.; Goh, M. C.; Eienthal, K. B. *J. Phys. Chem.* **1990**, *94*, 2222.
- (28) Heinz, T. F.; Tom, H. W. K.; Shen, Y. R. *Phys. Rev. A* **1983**, *28*, 1883.
- (29) Hicks, J. M., Ph.D. Dissertation, Columbia University, 1986.
- (30) Maroncelli, M.; Fleming, G. R. *J. Chem. Phys.* **1988**, *89*, 5044.
- (31) Walker, R. A.; Gragson, D. E.; Richmond, G. L. *Colloids and Surfaces A* **1999**, *154*, 175.
- (32) Du, Q.; Freysz, E.; Shen, Y. R. *Science* **1994**, *264*, 826.
- (33) Benjamin, I. *Chem. Rev.* **1996**, *96*, 1449; *Acc. Chem. Res.* **1995**, *28*, 233.